

# Nematic orders in Iron-based superconductors

Jiangping Hu<sup>a,b</sup>, Cenke Xu<sup>c</sup>

<sup>a</sup>*Department of Physics, Purdue University, West Lafayette, Indiana 47907, USA*

<sup>b</sup>*Beijing National Laboratory for Condensed Matter Physics, and Institute of Physics, Chinese Academy of Sciences, Beijing 100190, China*

<sup>c</sup>*Department of Physics, University of California, Santa Barbara, CA 93106*

---

## Abstract

In the newly discovered iron-based superconductors, many experiments have demonstrated the existence of the rotational symmetry breaking nematic order, which has been a prevailing phenomenon in many correlated electronic systems. In this paper, we review nematic behaviors in iron-pnictides and the mechanism behind the development of the nematic order. We discuss evidences that support the spin-driven nematicity in iron-pnictides. Theories, results and predictions will be discussed based on this picture. We also briefly discuss the generalization of this theory to the nematicity in iron-chalcogenides.

*Keywords:*

Iron-pnictides, Nematic order, antiferromagnet

---

## 1. Introduction

Microscopically, strongly correlated systems are usually described by extended Hubbard models with parameters such as Hubbard interaction, Hunds coupling, doping, etc. Despite the relatively simple microscopic models, the infrared physics of strongly correlated systems can be incredibly rich, various phases with completely different low energy descriptions can appear in the same phase diagram tuned by a few microscopic tuning parameters. Directly deriving the precise low energy phase diagram from the microscopic extended Hubbard models is usually tremendously difficult except for some special limits of the model. However, the competition and interplay between low energy phases can still be reasonably well described using effective theories that are based on some fundamental rules of physics. Many qualitative and semi-quantitative conclusions can be already drawn based on these low energy effective theories without the detailed information of the microscopic physics of the system.

Two decades after the discovery of the Cu-based superconductors (cuprates), a completely new class of high temperature superconductors was found, where the  $\text{Fe}^{2+}$  ions play the most important role [1, 2, 3, 4, 5, 6, 7]. Iron-based superconductors can be divided into two basic categories: iron-pnictides and iron-chalcogenides. The category of iron-pnictides includes many different families of materials which are named as

the 1111-family (example:  $\text{LaOFeAs}$ ) [1, 5, 7], the 111-family (example:  $\text{NaFeAs}$ ), the 122 family (example:  $\text{BaFe}_2\text{As}_2$ ) [8], and more complicated structures such as  $\text{Sr}_4\text{V}_2\text{O}_6\text{Fe}_2\text{As}_2$  [9]. Iron-chalcogenides include the 11 family  $\text{Fe/Se(Te)}$  [10] and the 122 family-alkali doped  $\text{A}_{1-x}\text{Fe}_{2-y}\text{Se}_2$  ( $\text{A} = \text{K, Cs, Rb}$ ) [11, 12, 13, 14]. The transition temperatures of these new superconductors reach as high as 56K [7] for iron-pnictides and 48K [15] for iron-chalcogenides.

The discovery of Fe-based superconductors provides a precious opportunity to investigate possible universalities shared in all of high temperature superconductors. Fe-based superconductors share many common features with cuprates. Both of them are quasi-two dimensional systems with a similar doping-dependent phase diagram involving strong antiferromagnetism (AF) [16]. Superconductivity is developed by introducing doping or applying pressure while long-range magnetic orders are suppressed (for a review, see Ref. [17]). Understanding the magnetism is thus pivotal to illustrate superconducting mechanism in these materials. While the relation between magnetism and superconductivity has been a central research focus in the past several years, here we review another important aspect of magnetism: electron nematicity, in undoped or under-doped iron based superconductors.

An electronic nematic liquid phase is characterized by rotational symmetry breaking. In the past decade,

this phase has been shown to appear almost universally in quasi-two dimensional electronic systems. The nematicity can arise from weakly correlated Fermi liquid systems dominated by kinetic energy to strongly correlated electron systems where electron-electron interactions are important. It has been observed throughout a variety of different electron systems including two-dimensional electron systems with high magnetic fields, strontium ruthenate materials and cuprates (for a review, see Ref. [18]).

In undoped or under-doped iron-pnictides, transport measurements reveal the existence of an intrinsic anisotropy of in-plane resistivity above magnetic Neel transition temperature  $T_N$ [19, 21], a strong evidence for the presence of an electronic nematic state. Similar anisotropy appears in a variety of experimental measurements, including local electronic structures measured by scanning tunneling microscopy (STM)[22], magnetic fluctuations by neutron scattering[23, 24], dynamic conductivity by optical reflection measurements [25] and electronic structures measured by angle resolved photoemission spectroscopy (ARPES) [26, 27] in de-twinned samples.

However, it is still controversial whether the observed anisotropies indicate an indisputable electronic nematic state. The debate arises because of the interplay between multi-degrees of freedom and the complexity of electronic structures in iron-pnictides. The lattice, spin, and orbital degrees of freedom all manifest themselves in the nematic state, which causes a debate on the origin of the rotational symmetry breaking of the tetragonal lattice. The magnetically ordered state in iron-pnictides is a collinear-AF (C-AF) state whose ordered wavevectors are  $(0, \pi)$  or  $(\pi, 0)$  with respect to the tetragonal iron lattice. The C-AF state not only breaks the  $SO(3)$  symmetry of the spin space, but also breaks the  $C^4$  rotational symmetry of the tetragonal lattice. Therefore, it is possible that an electronic nematic order which only breaks the latter  $C^4$  symmetry can be induced by magnetic fluctuations[28, 29]. Neutron scattering experiments have provided strong evidence showing that the magnetic fluctuations are indeed nematic above  $T_N$ [24]. However, the  $C^4$  rotational symmetry breaking can also be caused by other degrees of freedom. First, in iron-pnictides, the development of the C-AF order is always accompanied with a lattice structure distortion[16, 31]. A structural transition temperature  $T_s$  from the tetragonal lattice structure to an orthorhombic lattice structure is either at or above  $T_N$ , namely,  $T_s \geq T_N$ [16, 31]. Second, an onsite ferro-orbital order between  $d_{xz}$  and  $d_{yz}$  orbitals also breaks the same  $C^4$  rotational symmetry. Recently, such ferro-orbital order has been observed by

ARPES[26, 27] in pressure de-twinned samples. From standard symmetry argument, all the orders that break the same symmetry are allowed to be coupled directly with each other. Thus the existence of any one of them could lead to the presence of the others. Therefore, it is difficult to disentangle the role of the different degrees of freedom behind the rotational symmetry breaking.

This paper is to review the progress based on the spin-driven nematic order in Fe-pnictides materials. Before we start our review, we would like to discuss accumulative evidence supporting that the spin degree of freedom plays the dominant role in driving the rotational symmetry breaking. First, the lattice distortion observed throughout different families of iron-pnictides is rather small, much less than 1% of original lattice[16, 31]. Such a small lattice distortion can not cause a large change in electronic structures observed in the nematic state. Second, ferro-orbital ordering observed in ARPES[26, 27, 32] is also small and a separated ferro-orbital ordering transition is never observed. More importantly, the change of electronic structure in nematic state is not dominated by the  $d_{xz}$  and  $d_{yz}$  orbitals which can cause a  $C^4$  rotational symmetry breaking. Instead, all the orbitals act together and are equally important in the process of band reconstruction observed in the nematic state[33]. Third, even if the ordered magnetic moment in the C-AF state varies significantly in different families of iron-pnictides, the total magnetic moment obtained from inelastic neutron scattering is larger than over  $2.0\mu_B$  in underdoped samples[34, 24]. There is no question that the fluctuation of such a large moment can cause an electronic nematicity. Finally, as we will discuss in the paper, predictions derived from spin-driven mechanism are in a good agreement with experimental results[29, 28].

Iron-pnictides are metallic instead of insulating. However, electron-electron correlation has been proved to be very important. Experimentally, it has clearly shown that the nematicity in iron-pnictides is not a Pomeranchuk type instability characterized by Fermi surface deformation. Instead, in iron-pnictides, the entire band structure is reconstructed in the nematic state[35, 33], which suggests that it is not driven by the states near the Fermi surface, rather by all electrons due to correlation effects. These two facts lead to different approaches to study spin-driven nematicity. On one hand, being a metallic state, it is not surprising to treat the C-AF state as a spin density wave (SDW) state and formulate the nematicity based on the two SDW order parameters specified by order wavevectors  $(0, \pi)$  and  $(\pi, 0)$  respectively[37, 38]. On the other hand, due to the importance of electron-electron correlations as

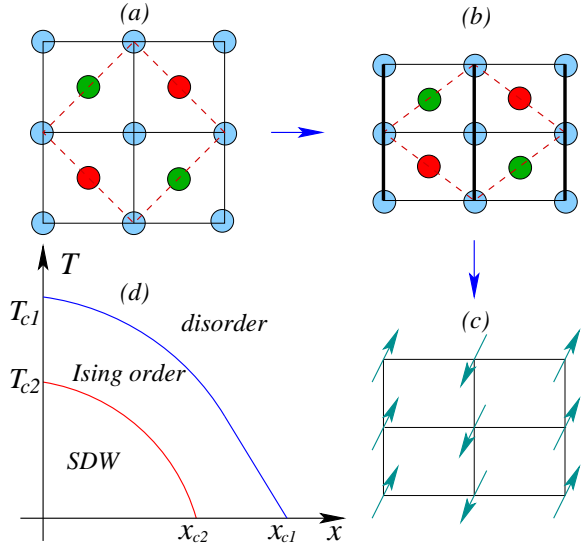


Figure 1: (a), the lattice structure of Fe-pnictides materials at room temperature. The gray circles are Fe ions, the green and red circles are As ions above and below the Fe plane, respectively. The dashed square is the two-Fe unit cell. (b), the lattice structure after the Ising nematic order is developed: the thick lines represent the bonds between parallel spins, but an Ising nematic order does not necessarily imply a nonzero long range spin order [16]. (c), the  $(0, \pi)$  spin order at low temperature. (d), the sketchy phase diagram for lattice distortion and C-AF (or SDW) as a function of temperature and doping  $x$ , for some of the Fe-pnictides materials. The blue curve represents the Ising transition, the red curve represents the C-AF transition.

well as the large magnetic moments observed in neutron scattering, we can take a local moment to formulate microscopic models based on short range exchange interactions[29, 28]. The nematic transition can be explicitly obtained and the nematicity can also be reflected in the magnetic exchange couplings. Fortunately, these two approaches result in an identical low energy Ginzburg-Landau effective action.

In this review paper, we will first take a phenomenological approach. We will discuss the field theory of the coupled nematic order and various aspects of the system at finite temperature, in particular, the nature of the phase transitions. Second, we will analyze microscopic models based on effective magnetic exchange couplings to obtain quantitative results and discuss the microscopic parameters that control the nematic transitions. Finally, we will discuss briefly nematic aspects of iron-chalcogenides, although at this stage it is still too early to write a complete review on these materials.

## 2. field theory of nematicity

### 2.1. Ginzburg-Landau field theory

Based on the observation discussed in the previous section, we first seek a phenomenological field theory description of the  $(\pi, 0)$ ,  $(0, \pi)$  C-AF (or SDW) and the nematic order. It was first proposed in Ref. [45, 46, 47] that the minimal spin model for the undoped parent Fe-pnictides material is either a  $S = 1$  or  $S = 2$  spin model with nearest and next-nearest neighbor couplings  $J_1, J_2$  that depend on the competition between the onsite Hubbard interaction, crystal field splitting, and the Hund's rule:

$$H = \sum_{\langle i, j \rangle} J_1 \vec{S}_i \cdot \vec{S}_j + \sum_{\langle\langle i, j \rangle\rangle} J_2 \vec{S}_i \cdot \vec{S}_j. \quad (1)$$

Unlike cuprates, in this system  $J_2$  is comparable with  $J_1$  because the As (or P) atoms are located at the plaquette center of the square lattice of magnetic Fe ions, rather than on the links. There is also a much weaker interlayer coupling  $J_z$ , which is necessary to stabilize the spin order. It is well-known that when  $J_1 < 2J_2$ , the classical ground state manifold of the model in Eq. 1 is  $S^2 \otimes S^2$ , because the two sublattices of the square lattice will each form a Néel order ( $\vec{\phi}_1$  and  $\vec{\phi}_2$ ), and the ground state energy is independent of the relative angle between these two Néel vectors. However, there is no generic symmetry of the system that protects the degeneracy within the classical  $S^2 \otimes S^2$  ground state manifold (GSM), thus quantum and thermal fluctuations will both lift the degeneracy, leading to parallel or antiparallel alignment of the two sublattice Néel vectors [48, 49, 50], thus the generic GSM of the system is  $S^2 \otimes Z_2$ , where the  $Z_2$  can be described by the Ising order parameter  $\sigma$  defined as follows:

$$\sigma \sim \vec{\phi}_1 \cdot \vec{\phi}_2. \quad (2)$$

We will defer the quantitative discussion of Eq. 1 to the next section, right now we will just discuss a Ginzburg-Landau theory for this lattice model. The lattice structure at high temperature has a perfect reflection symmetry  $P_{xy} : x \rightarrow y, y \rightarrow x$ , and under this transformation,  $\sigma$  always changes sign:  $\sigma \rightarrow -\sigma$ . Thus if  $\langle \sigma \rangle \neq 0$ , the reflection symmetry  $P_{xy}$  has to break, *i.e.* the system symmetry must reduce from tetragonal to orthorhombic.  $\sigma$  is precisely our nematic order parameter.

Based on the symmetry of the system, the minimal GL theory describing the C-AF and nematic order is [30]

$$F_{GL} = (\nabla_\mu \sigma)^2 + r_\sigma \sigma^2 + \sum_{a=1}^2 (\nabla_\mu \vec{\phi}_a)^2 + r_\phi |\vec{\phi}_a|^2$$

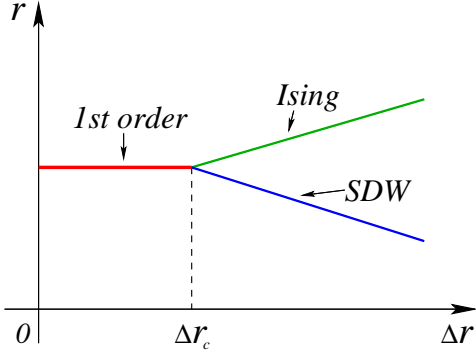


Figure 2: The schematic phase diagram of Ginzburg-Landau mean field theory in Eq. 3, plotted against  $r = r_\sigma + r_\phi$ , and  $\Delta r = r_\phi - r_\sigma$ .  $r$  is linear with temperature  $T$ , while  $\Delta r$  is tuned by anisotropy ratio  $J_z/J_{in}$ . When  $\Delta r$  is small, the interaction between  $\vec{\phi}_1$  and  $\vec{\phi}_2$  induces a strong first order transition, which corresponds to the undoped 122 materials with more isotropic electron kinetics; when  $\Delta r$  is large, the transition is split into two transitions, with an Ising transition followed by an magnetic transition at lower temperature, and this is the case in the 1111 materials with quasi two dimensional physics.

$$+ \tilde{u}\sigma\vec{\phi}_1 \cdot \vec{\phi}_2 + \dots \quad (3)$$

Roughly speaking,  $r_\sigma$  and  $r_\phi$  are tuned by the transition temperature for nematic and C-AF order respectively, large  $r$  corresponds to the high temperature disordered phase. The cubic coupling  $\tilde{u}$  in Eq. 3 implies that when  $\vec{\phi}_1$  and  $\vec{\phi}_2$  are ordered, the nematic order  $\sigma$  has to order; while the reverse is not necessarily true: there can be a phase with  $\sigma$  ordered while  $\vec{\phi}_a$  disordered.

By simply minimizing the GL theory, we obtain the phase diagram in Fig. 2: When  $\Delta r = r_\phi - r_\sigma$  is large, meaning  $\sigma$  has a much stronger tendency to order compared with  $\vec{\phi}_a$ , the system goes through two second order transitions associated with ordering of  $\sigma$  and  $\vec{\phi}_a$  respectively; while when  $\Delta r$  is small, the cubic coupling  $\tilde{u}$  in Eq. 3 merge the two transitions into one strong first order transition.

What does  $\Delta r$  correspond to in the real system? It is reasonable to start with a quasi two dimensional structure with interlayer spin coupling  $J_z$  much weaker than inplane couplings  $J_1 \sim J_2 \sim J$ . In Fe-pnicdides materials, the inplane coupling  $J$  is the energy scale that controls the ordering temperature of the Ising order parameter  $\sigma$ . However, for purely two dimensional systems, the O(3) C-AF is destroyed by thermal fluctuation at infinitesimal nonzero temperature, thus there is only one Ising transition at finite temperature for pure two dimensional system. With small  $J_z$ , the transition temperature of magnetic order scales as  $T_N \sim J/(\log J/J_z) \ll T_{ising}$ . Thus  $\Delta r$  is actually tuned by the effective dimensional-

ity of the system: When the system is more isotropic,  $\Delta r$  is smaller. The phase diagram of GL theory Eq. 3 is shown in Fig. 2.

Experiments have shown that in the 1111 materials, at finite temperature there are two second order transitions associated with lattice distortion and magnetic transition respectively [39]; while in undoped 122 materials there is only one strong first order transition where both phenomena occur simultaneously [40, 41, 42, 43, 44]. A simple Comparison between the experimental facts and our GL theory would imply that the 122 materials are more isotropic than 1111 materials. This is indeed true in real systems: First of all, the electron band structure calculated from LDA shows a much weaker  $z$  direction dispersion compared with the 122 samples [51]; also the upper critical field  $H_{c2}$  of 122 samples is much more isotropic [52]. This justifies treating the 1111 materials as a quasi two dimensional system, while treating the 122 materials as a three dimensional one. When  $J_z$  and  $J$  are close enough,  $\Delta r$  is small, and the coupling between the nematic order and the C-AF will drive the transition first order by minimizing the free energy Eq. 3.

## 2.2. finite temperature phase transitions

Now let us focus on the regime with large  $\Delta r$ , *i.e.* when there are two separate second order transitions at finite temperature. In principle, the transition of the Ising order parameter  $\sigma$  should belong to the 3D Ising Wilson-Fisher (WF) universality class, while the transition of the C-AF order parameter  $\vec{\phi}$  should belong to the 3d O(3) WF universality class. Thus at both transitions the specific heat should have a singularity peak. However, the specific heat measurement on  $\text{BaFe}_{2-x}\text{Co}_x\text{As}_2$  reveals two close but separate transitions at finite temperature, with a sharp peak at the C-AF transition, and a discontinuity at the lattice distortion transition [53]. A discontinuity of specific heat is a signature of mean field transition, in contrast to the sharp peak of Wilson-Fisher fixed point in 3 dimensional space.

Mean field transition can only be accurate for systems with spatial dimension equal to or higher than 4. Thus the specific heat measurement in Ref. [53] implies that effectively the dimension of the nematic transition is enhanced. In this section we will demonstrate that by coupling to the lattice strain field fluctuation, the effective spatial dimension  $D_{eff}$  for the nematic transition is enhanced to  $D_{eff} = 5$ , while the dimension for C-AF transition remains  $D_{eff} = 3$ .

Let us first investigate the C-AF transition. The C-AF transition at finite temperature should belong to the 3D O(3) transition if the lattice elasticity is ignored. The

O(3) order parameter  $\vec{\phi}$  couples to the lattice strain field with a quadratic term [54]:

$$|\vec{\phi}|^2(\partial_x u_x + \partial_y u_y + \lambda' \partial_z u_z). \quad (4)$$

After integrating out the displacement vector  $\vec{u}$ , this coupling generates a singular long range interaction between  $|\vec{\phi}|^2$  in the real space:

$$\int d^3 r d^3 r' g |\vec{\phi}|_r^2 \frac{f(\vec{r} - \vec{r}')}{|\vec{r} - \vec{r}'|^3} |\vec{\phi}|_{r'}^2. \quad (5)$$

$f$  is a dimensionless function which depends on the direction of  $\vec{r} - \vec{r}'$ . The scaling dimension of  $g$  is  $\Delta[g] = \alpha = 2/\nu - 3$ , and  $\nu$  is the standard exponent at the 3D O(3) transition, which is greater than  $2/3$  according to various types of numerical computations [55]. Therefore this long range interaction is irrelevant at the 3D O(3) transition, and by coupling to the strain field of the lattice, the C-AF transition is unaffected. However, if the C-AF has an Ising uniaxial anisotropy, the C-AF transition becomes a 3D Ising transition with  $\nu < 2/3$ , and the strain field would induce a relevant long range interaction [54], which leads to a run-away flow from the 3D Ising fixed point.

However, since the symmetry of the nematic order parameter  $\sigma$  is the same as the shear strain of the lattice, the strain tensor will couple to the Ising field  $\sigma$  as [30]

$$F_{\sigma, \vec{u}} = \tilde{\lambda} \sigma (\partial_x u_y + \partial_y u_x) + \dots \quad (6)$$

$\vec{u}$  is the displacement vector, the ellipses are all the elastic modulus terms. Notice that we have rotated the coordinates by 45 degree, since the true unit cell of the system is a two Iron unit cell (Fig. 2). After integrating out the displacement vector  $\vec{u}$ , the effective free energy of  $\sigma$  gains a new singular term at small momentum:

$$F_{\theta, \phi} \sim f(\theta, \phi) |\sigma_k|^2. \quad (7)$$

$f$  is a function of spherical coordinates  $\theta$  and  $\phi$  defined as  $(k_x, k_y, k_z) = k(\cos(\theta)\cos(\phi), \cos(\theta)\sin(\phi), \sin(\theta))$ , but  $f$  is independent of the magnitude of momentum  $\vec{k}$ . By tuning the uniform susceptibility  $r$ , at some spherical angle the minima of  $f$  reduces to zero, we will call these minima as nodal points. These nodal points are isolated from each other on the two dimension unit sphere labelled by  $\theta$ ,  $\phi$ , and are distributed on the unit sphere  $(\theta, \phi)$  according to the lattice symmetry.

The symmetry allows the minima to locate at the north and south pole, *i.e.*  $\theta = 0$  and  $\pi$ . Expanded at these two minima, the free energy reads

$$F = \int q^2 dq d\theta (q^2 + \lambda \theta^2 + r) |\sigma_{q, \theta}|^2 + O(\sigma^4) + \dots \quad (8)$$

The naive power counting shows that effectively the spatial dimension of this field theory Eq. 8 is  $D_{eff} = 5$ . The quartic coupling  $\sigma^4$  is irrelevant based on the straightforward power counting. Therefore the strain tensor fluctuation effectively increases the dimension by two, which drives the transition a mean field transition. This result is completely consistent with the specific heat measurement on  $\text{BaFe}_{2-x}\text{Co}_x\text{As}_2$ .

Using the Cartesian coordinate, the free energy Eq. 8 becomes:

$$F = \int dk_x dk_y dk_z \left( \frac{k_x^2 + k_y^2}{k_z^2} + k_z^2 + r \right) |\sigma_k|^2 + \dots \quad (9)$$

Based on this equation, the effective dimensions for momenta  $k_x$ ,  $k_y$  and  $k_z$  are

$$\Delta[k_x] = \Delta[k_y] = 2\Delta[k_z] = 2. \quad (10)$$

Thus the total dimension is still 5, considering  $\Delta[k_x] = \Delta[k_y] = 2\Delta[k_z] = 2$ . All the other momentum dependent terms in this free energy are irrelevant.

Based on the discussions above, we conclude that the lattice elasticity fluctuation will strongly modify the nature of the nematic transition, but will leave the C-AF transition unaffected. In Ref. [36], the authors proposed that when the two transitions are very close, the lattice fluctuation has the potential of driving the C-AF transition first order, because when these two transitions are very close the effective quartic term of the magnetic order parameter can become negative. This effect was also observed in experiments on lightly electron doped 122 materials in Ref. [20].

### 2.3. Hertz-Millis theory

In this subsection we will discuss the quantum critical points associated with nematic and C-AF orders [30]. A Hertz-Millis theory for quantum nematic order was studied in Ref. [56]. However, in our system the nematic order is strongly correlated with the spin interaction, thus the Hertz-Millis theory will be very different. The LDA calculation and photoemission both conclude that in the Brillouin zone of most Fe-pnictides materials, there are two hole pockets at the  $\Gamma$  point  $(0, 0)$ , and two electron pockets located at the M points  $((0, \pi)$  and  $(\pi, 0)$ ). Since the hole and electron pockets have different shapes, under translation of  $\vec{Q} = (\pi, 0)$  in the momentum space, the hole pocket will intersect with the electron pocket. This intersection leads to overdamping of the SDW order parameters. The decay rate can be calculated using Fermi's Golden rule:

$$\text{Im}[\chi(\omega, q)] \sim \int \frac{d^2 k}{(2\pi)^2} [f(\epsilon_{k+q}) - f(\epsilon_{k+\vec{Q}})]$$

$$\begin{aligned} & \times \delta(\omega - \epsilon_{k+q} + \epsilon_{k+\vec{Q}}) |k + Q|\vec{\phi}_{i,q}|k + q|^2 \\ & \sim c_0 \frac{\omega}{|\vec{v}_h \times \vec{v}_e|}. \end{aligned} \quad (11)$$

$v_h$  and  $v_e$  are the fermi velocity at the points on the hole and electron pockets which are connected by wave vector  $(\pi, 0)$ . The standard Hertz-Millis [57] formalism leads to a coupled  $z = 2$  theory in the Euclidean momentum space with Lagrangian

$$\begin{aligned} L_q &= \sum_{i=1}^2 \vec{\phi}_i \cdot (|\omega| + q^2 + r)\vec{\phi}_i + \gamma\vec{\phi}_1(q_x^2 - q_y^2) \cdot \vec{\phi}_2 + L', \\ L' &= \tilde{A}(|\vec{\phi}_1|^4 + |\vec{\phi}_2|^4) - \alpha(\vec{\phi}_1 \cdot \vec{\phi}_2)^2 + \tilde{C}|\vec{\phi}_1|^2|\vec{\phi}_2|^2. \end{aligned} \quad (12)$$

The parameter  $r$  can be tuned by pressure and doping. The Ising symmetry of  $\sigma = \vec{\phi}_1 \cdot \vec{\phi}_2$  on this system corresponds to transformation

$$\begin{aligned} x &\rightarrow y, y \rightarrow x, \\ \vec{\phi}_1 &\rightarrow \vec{\phi}_1, \vec{\phi}_2 \rightarrow -\vec{\phi}_2, \sigma \rightarrow -\sigma. \end{aligned} \quad (13)$$

This Ising symmetry excludes the term  $\vec{\phi}_1 \cdot \vec{\phi}_2$  in the Lagrangian, while the mixing term  $\gamma\vec{\phi}_1(q_x^2 - q_y^2) \cdot \vec{\phi}_2$  is allowed.

We can diagonalize the quadratic part of this Lagrangian by defining  $\vec{\phi}_A = (\vec{\phi}_1 + \vec{\phi}_2)/\sqrt{2}$  and  $\vec{\phi}_B = (\vec{\phi}_1 - \vec{\phi}_2)/\sqrt{2}$ :

$$\begin{aligned} L_q &= \vec{\phi}_A \cdot (|\omega| + (1 - \frac{\gamma}{2})q_x^2 + (1 + \frac{\gamma}{2})q_y^2 + r)\vec{\phi}_A \\ &+ \vec{\phi}_B \cdot (|\omega| + (1 + \frac{\gamma}{2})q_x^2 + (1 - \frac{\gamma}{2})q_y^2 + r)\vec{\phi}_B + L', \\ L' &= A(|\vec{\phi}_A|^4 + |\vec{\phi}_B|^4) + B(\vec{\phi}_A \cdot \vec{\phi}_B)^2 + C|\vec{\phi}_A|^2|\vec{\phi}_B|^2. \end{aligned} \quad (14)$$

After the redefinition, the Ising transformation becomes

$$\begin{aligned} x &\rightarrow y, y \rightarrow x, \\ \vec{\phi}_A &\rightarrow \vec{\phi}_B, \vec{\phi}_B \rightarrow -\vec{\phi}_A, \sigma \rightarrow -\sigma. \end{aligned} \quad (15)$$

Naively all three quartic terms  $A$ ,  $B$  and  $C$  are marginal perturbations on the  $z = 2$  mean field theory, a coupled renormalization group (RG) equation is required to determine the ultimate fate of these terms. Notice that the anisotropy of the dispersion of  $\vec{\phi}_A$  and  $\vec{\phi}_B$  cannot be eliminated by redefining space and time, therefore the number  $\gamma$  will enter the RG equation as a coefficient. The final coupled RG equation at the quadratic order for  $A$ ,  $B$  and  $C$  reads:

$$\frac{dA}{d \ln l} = -22A^2 - \frac{1}{2}B^2 - \frac{3}{2}C^2 - BC,$$

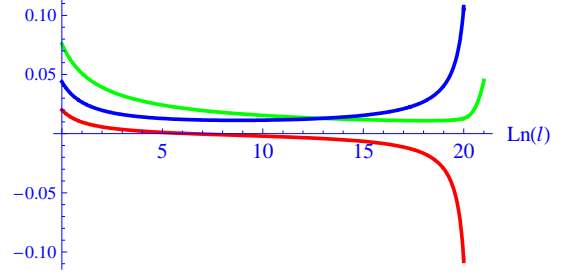


Figure 3: The solution of the RG equation Eq. 16. All three quartic perturbations decrease first, then increase and finally become non-perturbative. The run-away flow is weaker than marginally relevant perturbations.

$$\begin{aligned} \frac{dB}{d \ln l} &= -5uB^2 - 8AB - 8uBC, \\ \frac{dC}{d \ln l} &= -uB^2 - 4AB - 20AC - 4uC^2. \end{aligned} \quad (16)$$

$u$  is a smooth function of  $\gamma$ , which decreases smoothly from  $u = 1$  in the isotropic limit with  $\gamma = 0$ , to  $u = 0$  in the anisotropic limit with  $\gamma = 2$ . The self-energy correction of  $\vec{\phi}_a$  from the quartic terms will lead to the flow of the anisotropy ratio  $\gamma$  under RG, but this flow is at even higher order of the coupling constants, thus in our current discussion  $u$  is just taken a constant.

The typical solution of the RG equation Eq. 16 is plotted in Fig. 3, for the most natural choice of the initial values of parameters with  $\tilde{A} \gg \alpha$ ,  $\tilde{A} \gg \tilde{C}$  in Eq. 12 *i.e.* the coupling between  $\vec{\phi}_1$  and  $\vec{\phi}_2$  is weak. One can see that the three parameters  $A$ ,  $B$  and  $C$  all have run-away flows and eventually become nonperturbative. This run-away flow likely drives the transition weakly first order. However, the three coefficients will first decrease and then increase under RG flow. This behavior implies that this run-away flow is extremely weak, or more precisely even weaker than marginally relevant perturbations, because marginally relevant operators will still monotonically increase under RG flow, although increases slowly. Therefore in order to see this run-away flow, the correlation length has to be extremely long *i.e.* the system has to be very close to the transition, so the transition remains one single second order mean field transition for a very large length and energy range.

The interlayer coupling of  $\vec{\phi}_A$  and  $\vec{\phi}_B$  has so far been ignored, this is also a relevant perturbation at the  $z = 2$  mean field fixed point. The  $\hat{z}$  direction tunnelling is written as  $J_z \vec{\phi}_{a,z} \cdot \vec{\phi}_{a,z+1}$ , which has scaling dimension 2 at the  $z = 2$ ,  $d = 2$  mean field fixed point, and it becomes nonperturbative when

$$\frac{J_{in}}{J_z} \sim \left(\frac{\xi}{a}\right)^2 \sim r^{-1}. \quad (17)$$

This equation implies that if the tuning parameter  $r$  is in the small window  $r < J_z/J_{in}$ , the transition crossover back to a  $z = 2, d = 3$  transition, where all the quartic couplings are irrelevant. Since in the two dimensional theory these quartic terms are only very weakly relevant, in the end the interlayer coupling  $J_z$  may win the race of the RG flow, and this transition becomes one stable mean field second order transition.

### 3. Microscopic theory

#### 3.1. Model

As we have mentioned earlier, a simple microscopic model to capture the C-AF state is the  $J_1 - J_2 - J_z$  Heisenberg model. The interlayer coupling  $J_z$  must be included in order to address finite temperature magnetic transition. Moreover, as we will show later, the layer coupling  $J_z$  provides a control of the difference between nematic and magnetic transition temperatures. The Hamiltonian for such a model can be written as,

$$H = \sum_n [J_1 \sum_{\langle ij \rangle} \mathbf{S}_{i,n} \cdot \mathbf{S}_{j,n} + J_2 \sum_{\langle\langle ij \rangle\rangle} \mathbf{S}_{i,n} \cdot \mathbf{S}_{j,n} + J_z \sum_{n,i} \mathbf{S}_{i,n} \cdot \mathbf{S}_{i,n+1}], \quad (18)$$

where  $n$  is layer index. The spin nematic order which breaks the  $C^4$  rotational symmetry can be defined as

$$\sigma_i = \frac{1}{2} (\mathbf{S}_i \mathbf{S}_{i+\hat{x}} - \mathbf{S}_i \mathbf{S}_{i+\hat{y}}) \quad (19)$$

where  $\hat{x}$  and  $\hat{y}$  are unit vectors in a two dimensional tetragonal plane.

As we have mentioned in the introduction that both lattice distortion and ferro-orbital ordering which break the same  $C^4$  symmetry can be coupled to the spin nematic order. To be more specific, we consider the NN coupling  $J_1(|\mathbf{r}_i - \mathbf{r}_j|)$  as a function of the lattice distance between two sites. If there is a small orthorhombic lattice distortion  $\delta r$ , the NN coupling becomes

$$J_1(r_0 + \delta r/2) \mathbf{S}_i \mathbf{S}_{i+\hat{x}} + J_1(r_0 - \delta r/2) \mathbf{S}_i \mathbf{S}_{i+\hat{y}}. \quad (20)$$

where  $r_0$  is the lattice constant of the original tetragonal lattice. We can expand the above term and obtain a coupling between the lattice distortion and the nematic order,  $\lambda_{sl}(r_0) \delta r \sigma_i$ , where  $\lambda_{sl}(r) = \frac{\partial J_1(r)}{\partial r}$ . There is also coupling between the spin nematic order and an onsite orbital order between  $d_{xz}$  and  $d_{yz}$  orbitals. The coupling can be written as

$$\lambda_{so}(n_{xz}(i) - n_{yz}(i)) \sigma_i, \quad (21)$$

where  $n_{xz(yz)}(i)$  is electron density at the corresponding orbitals. If we include all these couplings and consider that the magnetism is the dominant player in the system, we can integrate out the above lattice and orbital fluctuations to obtain an effective pure magnetic term to account for the couplings. It is easy to show that such an integration leads to a biquadratic spin coupling limited to the NN bonds, namely,

$$H_q = - \sum_{\langle ij \rangle_{NN,n}} K (\mathbf{S}_{i,n} \cdot \mathbf{S}_{j,n})^2. \quad (22)$$

By adding such a term into the Hamiltonian in Eq.18 which will be called as the  $J_1 - J_2 - J_z - K$  model. The C-AF state is the ground state of the model when  $J_1 < 2J_2$  and  $K > 0$ . This extension has been recently considered in[59, 60].

#### 3.2. Large-S limit

We can exactly solve above model in the large S-limit. Without the  $K$  term, in the case of  $J_1 < 2J_2$ , the ground state is infinitely degenerate, as the relative angle between the spin directions on two sublattices is entirely arbitrary. If we consider quantum fluctuation, such a degeneracy will be broken. To show this, we can take Holstein-Primakoff transform for spin operators:

$$S_i^+ = \sqrt{2S} a_i \sqrt{1 - \frac{a_i^\dagger a_i}{2S}}, S_i^- = \sqrt{2S} a_i^\dagger \sqrt{1 - \frac{a_i^\dagger a_i}{2S}} \\ S_i^z = S - a_i^\dagger a_i, \quad (23)$$

where  $a_i$ 's are annihilation operators of spin wave bosons satisfying  $[a_i, a_j] = [a_i^\dagger, a_j^\dagger] = 0$  and  $[a_i, a_j^\dagger] = \delta_{ij}$ . We consider the following spin configuration in two sublattices: if a site  $(i_x, i_y)$  belongs to the first sublattice, its spin moment is  $\mathbf{S}_{1,i} = S(0, 0, (-1)^{i_x})$ ; if it belongs to the second sublattice, its spin moment is  $\mathbf{S}_{2,i} = S(-1)^{i_x}(\sin \theta, 0, \cos \theta)$ . Taking linear spin wave approximation in the Holstein-Primakoff transform, we have

$$S_{1,i}^+ = \sqrt{2S} \left( \frac{1 + (-1)^{i_x}}{2} a_i - \frac{1 - (-1)^{i_x}}{2} a_i^\dagger \right), \quad (24) \\ S_{1,i}^- = \sqrt{2S} \left( \frac{1 + (-1)^{i_x}}{2} a_i^\dagger - \frac{1 - (-1)^{i_x}}{2} a_i \right), \\ S_{1,i}^z = (-1)^{i_x} (S - a_i^\dagger a_i), \\ S_{2,i}^+ = (-1)^{i_x} \left( \sqrt{\frac{S}{2}} (a_i + a_i^\dagger) \cos \theta + (S - a_i^\dagger a_i) \sin \theta \right) \\ + \sqrt{\frac{S}{2}} (a_i - a_i^\dagger), \quad (25) \\ S_{2,i}^- = (-1)^{i_x} \left( \sqrt{\frac{S}{2}} (a_i + a_i^\dagger) \cos \theta + (S - a_i^\dagger a_i) \sin \theta \right)$$

$$-\sqrt{\frac{S}{2}}(a_i - a_i^\dagger), \quad (26)$$

$$S_{2,i}^z = (-1)^{i_x} \left( -\sqrt{\frac{S}{2}}(a_i + a_i^\dagger) \sin \theta + (S - a_i^\dagger a_i) \cos \theta \right).$$

Substituting these expressions into Eq.(18), and taking Fourier transformation, we obtain

$$H_{\pm}^{LSW} \sum_k [A_k a_k^\dagger a_k + \frac{B_k}{2}(a_k a_{-k} + h.c.)], \quad (27)$$

where

$$A_k = 4J_1 S + 4J_2 S + 2J_1 S [(1 + \cos \theta) \cos(k_x) + (1 - \cos \theta) \cos(k_y)] + 4J_z, \quad (28)$$

$$B_k = -\{2J_1 S [(1 - \cos \theta) \cos(k_x) + (1 + \cos \theta) \cos(k_y)] + 2J_2 S (\cos(k_x + k_y) + \cos(k_x - k_y)) + 4J_z \cos(k_z)\}. \quad (29)$$

Taking the Bogliubov transform for bosons, we obtain

$$H^{LSW} = \sum_k (\gamma_k^\dagger \gamma_k + \frac{1}{2}) \omega_k, \quad (30)$$

where

$$\omega_k = \sqrt{A_k^2 - B_k^2}, \quad (31)$$

and  $\gamma_k = \cosh \psi_k a_k + \sinh \psi_k a_{-k}^\dagger$ ,  $\gamma_k^\dagger = \cosh \psi_k a_k^\dagger + \sinh \psi_k a_{-k}$ , and  $\tanh(2\psi_k) = -\frac{B_k}{A_k}$ . At zero temperature for small  $J_z$ , the quantum fluctuation contributes a zero-point energy for bosons

$$E_0^Q = \frac{1}{2} \sum_k \omega_k = -\frac{\gamma_Q S J_1^2}{4J_2} \cos^2 \theta + J_2 O\left(\left(\frac{J_1}{J_2}\right)^4\right), \quad (32)$$

where  $\gamma_Q = 0.13$ . The ground state, therefore, is either  $\theta = 0$  or  $\theta = \pi$ , which means that spins in two sublattice are collinearly aligned, namely, the C-AF state. The collinear configuration is an effect of spin fluctuation. This effect is called ‘‘order by disorder’’ [48, 49, 50].

The energy in Eq.32 can be taken into account by the bi-quadratic  $K$  term as well. The quantum fluctuation contribution to the value of  $K$  is given by  $\frac{\gamma_Q J_1^2}{8S^3 J_2}$ . We can thus view the  $K$  term in the  $J_1 - J_2 - J_z - K$  model as an effective term that includes contributions from all different couplings. In the C-AF state, the  $K$  term can be decoupled as

$$H_Q = -2 \sum_{\langle ij \rangle_{NN,n}} K \sigma_{ij,n} (\mathbf{S}_{i,n} \cdot \mathbf{S}_{j,n}) + \text{cons.} \quad (33)$$

where  $\sigma_{ij,n} = \langle \mathbf{S}_{i,n} \cdot \mathbf{S}_{j,n} \rangle = \pm \sigma$ , is the expectation value of the spin-spin interaction in the C-AF state. The sign

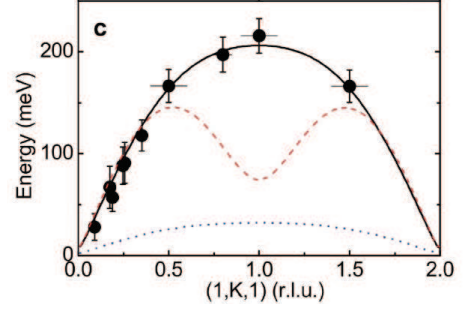


Figure 4: The spin wave dispersion along  $(\pi, k, \pi)$  direction reported in[23]: the solid line is fitted when  $J_{1a} \gg J_{1b}$  and the dashed line is fitted if  $J_{1a} \sim J_{1b}$ .

is chosen to be positive if the spins are FM along one axis (b-axis) and negative if they are AF along the other axis (a-axis) in the C-AF state. Combining this term with  $J_1$  term in the original Hamiltonian, the effective nearest neighbour exchange couplings in the C-AF State become

$$J_{1a} = J_1 + 2K\sigma, J_{1b} = J_1 - 2K\sigma. \quad (34)$$

Thus, the spin wave excitations in the C-AF state are effectively described by a  $J_{1a} - J_{1b} - J_2 - J_z$  model.

Experimentally, a large difference between  $J_{1a}$  and  $J_{1b}$  is indeed observed in the C-AF state[61, 23, 24]. The spin wave energy at wavevector  $(\pi, \pi, \pi)$  is very sensitive to the difference between  $J_{1a}$  and  $J_{1b}$ . The energy is proportional to  $\sqrt{J_{1a} - J_{1b}}$ . Experimentally, The gap  $\omega(\pi, \pi, \pi)$  measured in the 122 family has been very large as shown in fig.4, namely, the difference of  $J_{1a}$  and  $J_{1b}$  is very large. Such a large difference suggests a strong nematic order and a sizable  $K$  value.

### 3.3. large- $N$ limit

The model can be analytically solved in the large- $N$  limit to obtain phase diagram and transition temperature. We take the continuum limit following the derivation in [62, 60]. The low energy effective Hamiltonian reads

$$H_{eff} = \int d^2 r \sum_{n,\alpha} [\tilde{J}_2 |\nabla \mathbf{n}_{\alpha,n}|^2 - \tilde{J}_z \mathbf{n}_{\alpha,n} \cdot \mathbf{n}_{n+1,\alpha}] - \tilde{K} \sum_n [\mathbf{n}_{1,n} \cdot \mathbf{n}_{2,n}]^2 + \frac{\tilde{J}_1}{2} \sum_n \mathbf{n}_{1,n} \cdot \partial_x \partial_y \mathbf{n}_{2,n} \quad (35)$$

where  $\tilde{J}_i = J_i S^2$ ,  $\tilde{K} = KS^4/2$  and  $\mathbf{n}_{1(2),n}$  are AF orders in the two sublattices mentioned earlier respectively and

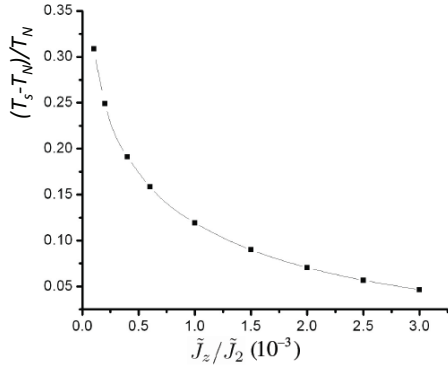
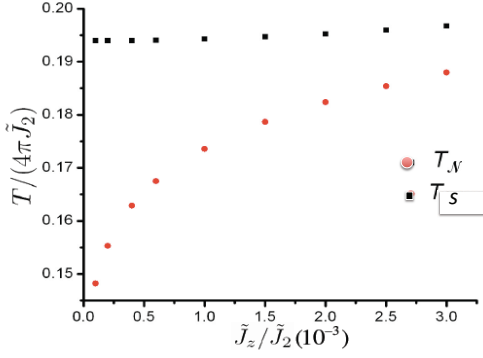


Figure 5: Left:  $T_S$  and  $T_N$  as the function of  $\tilde{J}_z$  for  $\tilde{J}_2 = 2\tilde{J}_1$  and  $N = 3$ . Right:  $\frac{T_S - T_N}{T_N}$  as the function of  $\tilde{J}_z$  for  $\tilde{J}_1 = 0.5\tilde{J}_2$ .

the nematic order in the continuum limit becomes  $\sigma = \mathbf{n}_{1,n} \cdot \mathbf{n}_{2,n}$ . We can solve the effective model in the large- $N$  limit analytically. In general, there are two transition temperatures. The nematic transition temperature  $T_S$  is analytically given by

$$\frac{4\pi\tilde{J}_2}{NT_S} = \ln \frac{\tilde{J}_2/(NT_S)}{\sqrt{\left(\frac{\tilde{K}}{4\pi\tilde{J}_2}\right)^2 + \left(\frac{\tilde{J}_z}{NT_S}\right)^2 + \frac{\tilde{K}}{4\pi\tilde{J}_2}}}, \quad (36)$$

and the C-AF transition temperatures,  $T_N$  is determined by,

$$\frac{\sigma_c}{2\tilde{K}} = \frac{1}{8\pi\tilde{J}_2} \ln \frac{\sigma_c + \frac{\tilde{J}_z}{NT_N} + 2\sqrt{\frac{\sigma_c^2}{4} + \frac{\sigma_c\tilde{J}_z}{NT_N}}}{\tilde{J}_z/(NT_N)},$$

$$\frac{\sigma_c}{2\tilde{K}} + \frac{1}{NT_N} = \frac{1}{4\pi\tilde{J}_2} \ln \frac{\tilde{J}_2}{\tilde{J}_z}. \quad (37)$$

$T_N$  is always lower than  $T_S$  in the solutions of above equations. Moreover,  $T_N = 0$  if  $\tilde{J}_z = 0$ , and is finite

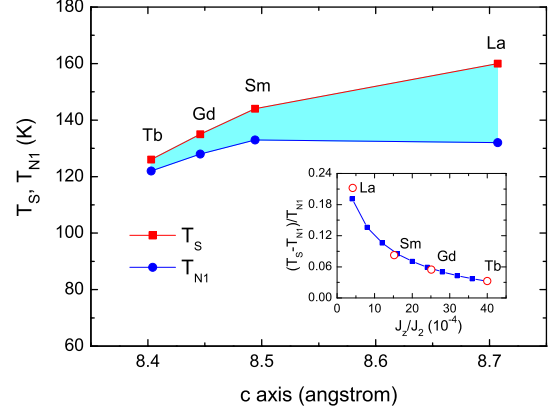


Figure 6: Plot of structural phase transition temperature  $T_S$ , and magnetic transition temperature  $T_N$  associated to the AF order of Fe ions, versus the c-axis for RFeAsO (R = La, Sm, Gd, Tb). Inset: plot of  $(T_S - T_N)/T_N$  versus  $J_z/J_2$ . The open circles denote the experimental data of  $(T_S - T_N)/T_N$ , and the solid squares denote the theoretical values[63].

otherwise. For small  $J_z$ , one can approximately have  $T_N \sim \tilde{J}_2 / \ln(\frac{\tilde{J}_2}{T_N})$ . In fig.5, we plot the two transition temperatures and their difference as the function of  $J_z/J_2$ . The difference decreases as  $J_z$  increases. This qualitative prediction is consistent with the GL field theory approach discussed in the previous section, and it is also confirmed in the 1111 family[63] as shown in fig.6.

This calculation shows that as soon as  $J_z$  is much larger than  $10^{-3}J_z$ , the two transitions are close to each other so that they become practically inseparable in experiments. This result is consistent with the fact there is only one phase transition in the parent compounds of the 122 families where  $J_z$  determined by spin wave excitations is rather large: in  $\text{CaFe}_2\text{Se}_2$ ,  $J_z$  is almost one third of the in-plane coupling  $J_2$ [23]. In  $\text{BaFe}_2\text{As}_2$ ,  $J_z$  is about  $0.015J_2$ [24]. The prediction is further confirmed in under-doped 122 materials. Upon electron doping in  $\text{BaFe}_2\text{As}_2$ , for example,  $\text{BaFe}_{2-x}\text{Ni}_x\text{As}_2$ [64], the spin excitations become much less three dimensional. The effective  $J_z$  is drastically reduced and two phase transitions were observed.

#### 4. Nematic order in Iron-Chalcogenides

Iron-chalcogenides include two families, the 11 family (FeTe/Se) and the 122 family ( $\text{A}_{1-x}\text{Fe}_{2-y}\text{Se}_2$  (A = K, Rb, Cs)). While the former shares similar band structures with iron-pnictides, the latter exhibits several

distinct characters that are noticeably absent in other iron-based superconductors, including the absence of hole pockets at  $\Gamma$  point of Brillouin zone in their superconducting (SC) phases[65, 66, 67], AF ordered insulating phases[68, 69, 70] with very high Néel transition temperatures in their parental compounds[13] and intrinsic vacancy ordering. These intriguing properties have stimulated many exciting research activities.

While it is too early to call a reasonable review for iron-chalcogenides, the magnetic orders in the parent compounds of these two families have been measured. Unlike iron-pnictides whose different families share a common C-AF state, different families of iron-chalcogenides exhibit different magnetically ordered states. The FeTe compounds of the 11 family has a bicollinear AF(B-CAF) ground state as shown in fig.7(a). The B-CAF state is accompanied by a monoclinic lattice distortion. The distortion can produce 1.3% change of the tetragonal lattice constant, a value much larger than the orthorhombic distortion in iron-pnictides[71]. The large lattice distortion indicates a strong coupling between spin and lattice and is consistent with the fact there is only one strong first-order type transition in FeTe, namely, the B-CAF and monoclinic lattice distortion take place at the same transition temperature which is about 70K[72]. The ordered magnetic moment in FeTe about  $2.3\mu_B$  is also significantly larger than the ones in iron-pnictides.

For the 122 family,  $R_{1-x}Fe_{2-y}Se_2$ , one magnetically ordered state with iron vacancy order, called block-AF<sub>v</sub>, has been identified when  $x = 0.8$  and  $y = 0.4$  as shown in fig.7(b). Iron vacancies form a  $\sqrt{5} \times \sqrt{5}$  pattern and four iron spins group together to form a super-site with ferromagnetic(FM) alignment. In the lattice formed by the super-sites, it is AF ordered. The ordered moment per iron site in the B-AF<sub>v</sub> state reaches  $3.3\mu_B$  and the transition temperature is about 500k[68, 69]. The lattice distortion in the B-AF<sub>v</sub> state can reach 2% of the original lattice constant. More importantly, the B-AF<sub>v</sub> state is insulating with a gap larger than  $0.3eV$ . It is the first insulating state observed in iron-based superconductors.

Recently, it has been shown that the effective magnetic exchange models that describe different ordered states can be unified into a  $J_1 - J_2 - J_3 - K - J_z$  model[73, 74, 60], where  $J_3$  is the next next nearest neighbour magnetic exchange coupling. Compared to the  $J_1 - J_2 - K - J_z$  model for iron-pnictides, there are two major differences:  $J_1$  is strong ferromagnetic (FM) in iron chalcogenides and  $J_3$  is significant and AF. Without vacancy, the model has two degenerate classical ground states: the B-CAF or bloch-AF (B-AF) state which is shown in fig.7(c). An effective theory based

on this model has been discussed in [75]. The complete field description of the  $J_1 - J_2 - J_3 - J_c - K$  model near the B-CAF or B-AF phase is given by  $H_T = H_B + H_K$  where

$$H_B = \int d^2\mathbf{r} \sum_{n,\alpha} \left[ \frac{1}{2} J_3 |\nabla \vec{\phi}_{n,\alpha}(\mathbf{r})|^2 - J_c \vec{\phi}_{n,\alpha}(\mathbf{r}) \cdot \vec{\phi}_{n+1,\alpha}(\mathbf{r}) \right] - g' \sum_n \{ [\vec{\phi}_{n,1}(\mathbf{r}) \cdot \vec{\phi}_{n,3}(\mathbf{r})]^2 + [\vec{\phi}_{n,2}(\mathbf{r}) \cdot \vec{\phi}_{n,4}(\mathbf{r})]^2 \}, \quad (38)$$

and

$$H_K = -K \int d^2\mathbf{r} \sum_n \{ [\vec{\phi}_{n,1}(\mathbf{r}) \cdot \vec{\phi}_{n,2}(\mathbf{r})]^2 \quad (39)$$

$$+ [\vec{\phi}_{n,1}(\mathbf{r}) \cdot \vec{\phi}_{n,4}(\mathbf{r})]^2 + [\vec{\phi}_{n,2}(\mathbf{r}) \cdot \vec{\phi}_{n,3}(\mathbf{r})]^2 + [\vec{\phi}_{n,3}(\mathbf{r}) \cdot \vec{\phi}_{n,4}(\mathbf{r})]^2 \} \quad (40)$$

where  $\vec{\phi}_{n,\alpha}$  with  $\alpha = 1, 2, 3, 4$  are four Neel order parameters defined in the four sublattices of the tetragonal lattice specified by the  $J_3$  coupling and  $g' \sim 0.13J_2^2/J_3$ . In this model, there are four independent Ising orders  $\sigma_1 = g' \vec{\phi}_{n,1}(\mathbf{r}) \cdot \vec{\phi}_{n,3}(\mathbf{r})$ ,  $\sigma_2 = g' \vec{\phi}_{n,2}(\mathbf{r}) \cdot \vec{\phi}_{n,4}(\mathbf{r})$ ,  $\sigma_+ = K(\vec{\phi}_{n,1}(\mathbf{r}) + \vec{\phi}_{n,3}(\mathbf{r})) \cdot (\vec{\phi}_{n,2}(\mathbf{r}) + \vec{\phi}_{n,4}(\mathbf{r}))$  and  $\sigma_- = K(\vec{\phi}_{n,1}(\mathbf{r}) - \vec{\phi}_{n,3}(\mathbf{r})) \cdot (\vec{\phi}_{n,2}(\mathbf{r}) - \vec{\phi}_{n,4}(\mathbf{r}))$ .  $\sigma_+$  and  $\sigma_-$  describe the Ising orders associated with the B-AF and B-CAF phases respectively. The Ising order  $\sigma_1$  breaks rotational symmetry and represents a nematic phase. The analysis of this effective field theory has been carried out in[75, 60]. This effective theory also suggests that the lattice-spin coupling is extremely important in determining the true magnetic order in iron-chalcogenides due to intrinsic magnetic frustration.

Since there are few experiments that have been implemented to probe the nematic nature of the B-CAF state explicitly, we will not extend our discussion further here. However, it is interesting to point out that since the 122 family of iron-chalcogenides may approach a magnetically ordered insulating phase, the materials may carry similar nematic phases as curpates upon doping. The charge degree of freedom hence may manifest itself and play an important role in driving nematicity in these new materials.

## 5. Summary and Extensions

In this article we reviewed the study of the electronic nematic order and the C-AF order that have been universally observed in iron-pnictides materials. Based on the experimental observation of the close relation between these two order parameters, we propose the theory of spin interaction driven nematic order in these materials.

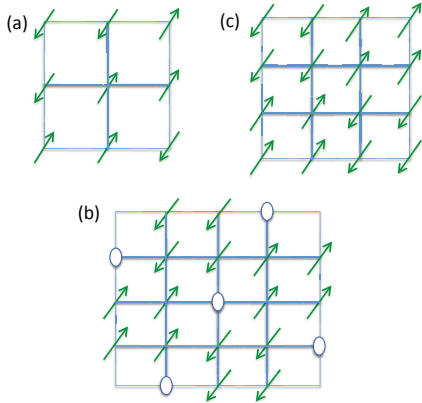


Figure 7: Sketch of spin configurations of (a) bi-collinear AF (B-CAF) state observed in FeTe, (b) block AF with vacancy order (B-AF<sub>v</sub>) observed in K<sub>0.8</sub>Fe<sub>1.6</sub>Se<sub>2</sub>, and (c) block AF order (B-AF) order.

In this article we have thoroughly studied this problem with both low energy field theories such as Ginzburg-Landau theory and Hertz-Millis theory, and also microscopic theories in the large- $S$  and large- $N$  limit. We also briefly discussed the generalization of this picture to iron-chalcogenides materials.

A proof of the nematic order induced by spin interactions can have strong impact on the field. It would automatically suggest that the superconductivity mechanism is most likely to be magnetically driven. While both experiments and theories reviewed here have provided convincing evidence, we agree that the debate over the origin of the rotational symmetry breaking has not been fully settled at this stage.

Although we have a detailed theory of the interplay of electron nematicity and spin order, the relation between these order parameters and the high temperature superconductor is still unclear. Strong competition between spin orders and superconductor phase has been observed experimentally in iron-pnictides, meaning that a complete description of low energy physics should also involve the superconducting phase. This is one of the directions that can be pursued in the future.

In section II, we have seen that the lattice strain field fluctuation strongly affects the finite temperature phase transition of the nematic order. However, in section II the discussion of the lattice strain field was purely classical and phenomenological. At zero temperature, the nematic order will conceivably strongly couple to the phonon modes of the lattice, thus the phonon fluctuation will most likely also strongly affect the quantum critical behavior, as long as the spin wave excitation at zero temperature. A complete theory including the phonon

of the lattice will significantly enrich the physics.

The 122 family of iron-chalcogenides has opened a new chapter in the field. It provides a fresh ground to test the concept of nematism. Since electron-electron correlation is generally believed to be stronger in iron-chalcogenides than iron-pnictides, exciting results related to nematism in the future can be expected.

*Acknowledge:* We thank S. Kivelson, S. Sachdev, C. Fang, Pengcheng Dai, Donglei Feng and X.H. Chen for many valuable discussions.

## References

- [1] Y. Kamihara, T. Watanabe, M. Hirano, and H. Hosono, *J. Am. Chem. Soc.* **130**, 3296 (2008).
- [2] G. Mu, X. Zhu, L. Fang, L. Shan, C. Ren, and H.-H. Wen, *Chin. Phys. Lett.* **25**, 2221 (2008).
- [3] H.-H. Wen, G. Mu, L. Fang, H. Yang, and X. Zhu, *Europhys. Lett.* **82**, 17009 (2008).
- [4] J. Dong, H. J. Zhang, G. Xu, Z. Li, G. Li, W. Z. Hu, D. Wu, G. F. Chen, X. Dai, J. L. Luo, et al., *Europhysics Letters* **83**, 27006 (2008).
- [5] X. H. Chen, T. Wu, G. Wu, R. H. Liu, H. Chen, and D. F. Fang, *Nature* **453**, 761 (2008).
- [6] G. F. Chen, Z. Li, D. Wu, G. Li, W. Z. Hu, J. Dong, P. Zheng, J. L. Luo, and N. L. Wang, *Phys. Rev. Lett.* **100**, 247002 (2008).
- [7] Z.-A. Ren, J. Yang, W. Lu, W. Yi, G.-C. Che, X.-L. Dong, L.-L. Sun, and Z.-X. Zhao, *Materials Research Innovations* **12**, 105 (2008).
- [8] M. Rotter, M. Tegel, and D. Johrendt, *Physical Review Letters* **101**, 107006 (2008).
- [9] X. Zhu and e. al., *Phys. Rev. B* **79**, 220512 (2009).
- [10] F.-C. Hsu, J.-Y. Luo, K.-W. Yeh, T.-K. Chen, T.-W. Huang, P. M. Wu, Y.-C. Lee, Y.-L. Huang, Y.-Y. Chu, D.-C. Yan, et al., *PNAS* **105**, 14262 (2008), ISSN 0027-8424.
- [11] J. Guo, S. Jin, G. Wang, S. Wang, K. Zhu, T. Zhou, M. He, and X. Chen, *Physical Review B* **82**, 180520 (2010).
- [12] M.-H. Fang, H.-D. Wang, C.-H. Dong, Z.-J. Li, C.-M. Feng, J. Chen, and H. Q. Yuan, *Europhysics Letters* **94**, 27009 (2011).
- [13] R. H. Liu, X. G. Luo, M. Zhang, A. F. Wang, J. J. Ying, X. F. Wang, Y. J. Yan, Z. J. Xiang, P. Cheng, G. J. Ye, et al., *Europhysics Letters* **94**, 27008 (2011).
- [14] Y. J. Yan, M. Zhang, A. F. Wang, J. J. Ying, Z. Y. Li, W. Qin, X. G. Luo, J. Q. Li, J. Hu, and X. H. Chen, *Arxiv:1104.4941* (2011).
- [15] L. Sun, X.-J. Chen, J. Guo, P. Gao, H. Wang, M. Fang, X. Chen, G. Chen, Q. Wu, C. Zhang, et al., *Arxiv:1110.2600* (2011).
- [16] C. de la Cruz, Q. Huang, J. W. Lynn, J. Li, W. R. II, J. L. Zarestky, H. A. Mook, G. F. Chen, J. L. Luo, N. L. Wang, et al., *Nature* **453**, 899 (2008).
- [17] D. Johnston, *Advances in Physics* **59**, 803 (2010).
- [18] E. Fradkin, S. A. Kivelson, M. J. Lawler, J. P. Eisenstein, and A. P. Mackenzie, *Annual Review of Condensed Matter Physics* **1**, 153 (2010).
- [19] I. R. Fisher, L. Degiorgi, and Z. X. Shen, *Reports on Progress in Physics* **74**, 124506 (2011).
- [20] M. G. Kim, R. M. Fernandes, A. Kreyssig, J. W. Kim, A. Thaler, S. L. Bud'ko, P. C. Canfield, R. J. McQueeney, J. Schmalian, and A. I. Goldman, *Phys. Rev. B* **83**, 134522 (2011).
- [21] J. J. Ying, X. F. Wang, T. Wu, Z. J. Xiang, R. H. Liu, Y. J. Yan, A. F. Wang, M. Zhang, G. J. Ye, P. Cheng, et al., *Physical Review Letters* **107**, 067001 (2011).

- [22] T.-M. Chuang, M. P. Allan, J. Lee, Y. Xie, N. Ni, S. L. Bud'ko, G. S. Boebinger, P. C. Canfield, and J. C. Davis, *Science* **327**, 181 (2010).
- [23] J. Zhao, D. T. Adroja, D. X. Yao, R. Bewley, S. L. Li, X. F. Wang, G. Wu, X. H. Chen, J. P. Hu, and P. C. Dai, *Nature Physics* **5**, 555 (2009).
- [24] L. W. Harriger, H. Luo, M. Liu, T. G. Perring, C. Frost, J. Hu, M. R. Norman, and P. Dai, *Phys. Rev. B* **84**, 054544 (2010).
- [25] M. Nakajima, T. Liang, S. Ishida, Y. Tomioka, K. Kihou, C. H. Lee, A. Iyo, H. Eisaki, T. Kakeshita, T. Ito, et al., *PNAS* **108**, 12238 (2011).
- [26] M. Yi, D. H. Lu, J.-H. Chu, J. G. Analytis, A. P. Sorini, A. F. Kemper, S.-K. Mo, R. G. Moore, M. Hashimoto, W. S. Lee, et al., *ArXiv:1011.0050* (2011).
- [27] M. Yi, D. H. Lu, R. G. Moore, K. Kihou, C.-H. Lee, A. Iyo, H. Eisaki, T. Yoshida, A. Fujimori, and Z.-X. Shen, *Arxiv:1116134* (2011).
- [28] C. Fang, H. Yao, W.-F. Tsai, J. Hu, and S. A. Kivelson, *Phys. Rev. B* **77**, 224509 (2008).
- [29] C. Xu, M. Mueller, , and S. Sachdev, *Phys. Rev. B* **78**, 20501 (2008).
- [30] Y. Qi and C. Xu, *Phys. Rev. B* **80**, 094402 (2009).
- [31] J. Zhao, Q. Huang, C. de la Cruz, S. Li, J. W. Lynn, Y. Chen, M. A. Green, G. F. Chen, G. Li, Z. Li, et al., *Nature Materials* **7**, 953 (2008).
- [32] Y. Zhang, C. He, Z. R. Ye, J. Jiang, F. Chen, M. Xu, Q. Q. Ge, B. P. Xie, J. Wei, M. Aeschlimann, et al., *arXiv:1111.6430* (2011).
- [33] C. He, Y. Zhang, B. P. Xie, X. F. Wang, L. X. Yang, B. Zhou, F. Chen, M. Arita, K. Shimada, H. Namatame, et al., *Physical Review Letters* **105**, (2010).
- [34] M. Wang, X. C. Wang, D. L. Abernathy, L. W. Harriger, H. Q. Luo, Y. Zhao, J. W. Lynn, Q. Q. Liu, C. Q. Jin, C. Fang, et al., *Phys. Rev. B* **83**, 220515(R) (2011).
- [35] L. X. Yang, Y. Zhang, H. W. Ou, J. F. Zhao, D. W. Shen, B. Zhou, J. Wei, F. Chen, M. Xu, C. He, et al., *Physical Review Letters* **102** (2009).
- [36] A. Cano, M. Civelli, I. Eremin, and I. Paul, *Phys. Rev. B* **82**, 020408(R) (2010).
- [37] I. Eremin and A. V. Chubukov, *Physical Review B* **81**, 24511 (2010).
- [38] R. M. Fernandes, L. H. Vanbeber, S. Bhattacharya, P. Chandra, V. Keppens, D. Mandrus, M. A. McGuire, B. C. Sales, A. S. Sefat, and J. Schmalian, *Physical Review Letters* **105**, 157003 (2010).
- [39] M. A. McGuire, A. D. Christianson, A. S. Sefat, B. C. Sales, M. D. Lumsden, R. Jin, E. A. Payzant, D. Mandrus, Y. Luan, V. Keppens, et al., *Phys. Rev. B* **78**, 094517 (2008).
- [40] Q. Huang, Y. Qiu, W. Bao, J. W. Lynn, M. A. Green, Y. Chen, T. Wu, G. Wu, and X. H. Chen, *Phys. Rev. Lett.* **101**, 257003 (2008).
- [41] C. Krellner, N. Caroca-Canales, A. Jesche, H. Rosner, A. Ormeci, and C. Geibel, *Phys. Rev. B* **78**, 100504(R) (2008).
- [42] J.-Q. Yan, A. Kreyssig, S. Nandi, N. Ni, S. L. Bud'ko, A. Kracher, R. J. McQueeney, R. W. McCallum, T. A. Lograsso, A. I. Goldman, et al., *Phys. Rev. B* **78**, 024516 (2008).
- [43] J. Zhao, W. R. II, J. W. Lynn, G. F. Chen, J. L. Luo, N. L. Wang, J. Hu, and P. Dai, *Phys. Rev. B* **78**, 014504(R) (2008).
- [44] A. I. Goldman, D. N. Argyriou, B. Ouladdiaf, T. Chatterji, A. Kreyssig, S. Nandi, N. Ni, S. L. Bud'ko, P. Canfield, and R. J. McQueeney, *Phys. Rev. B* **78**, 100506(R) (2008).
- [45] Q. Si and E. Abrahams, *Phys. Rev. Lett.* **101**, 076401 (2008).
- [46] F. Ma, Z.-Y. Lu, and T. Xiang, *Physical Review B* **78**, 224517 (2008).
- [47] T. Yildirim, *Physical Review Letters* **101**, 57010 (2008).
- [48] C. L. Henley, *Phys. Rev. Lett.* **62**, 2056 (1989).
- [49] P. Chandra, P. Coleman, and A. I. Larkin, *Phys. Rev. Lett.* **64**, 88 (1990).
- [50] N. Read and S. Sachdev, *Phys. Rev. Lett.* **66**, 1773 (1991).
- [51] F. Ma, Z.-Y. Lu, and T. Xiang, *Front. Phys. China* **5**, 150 (2010).
- [52] H. Q. Yuan, J. Singleton, F. F. Balakirev, G. F. Chen, J. L. Luo, and N. L. Wang, *Nature* **457**, 565 (2009).
- [53] J.-H. Chu, J. G. Analytis, C. Kucharczyk, and I. R. Fisher, *Phys. Rev. B* **78**, 014506 (2009).
- [54] D. Bergman and B. I. Halperin, *Phys. Rev. B* **13**, 2145 (1976).
- [55] P. Calabrese, A. Pelissetto, and E. Vicari (2003), *cond-mat/0306273*.
- [56] V. Oganesyan, S. Kivelson, and E. Fradkin, *Phys. Rev. B* **64**, 195109 (2001).
- [57] J. A. Hertz, *Phys. Rev. B* **14**, 1165 (1976).
- [58] L. Zhu, M. Garst, A. Rosch, and Q. Si, *Phys. Rev. Lett.* **91**, 066404 (2003).
- [59] A. L. Wysocki, K. D. Belashchenko, and V. P. Antropov, *Nature Physics* **7**, 485 (2011).
- [60] J. Hu, B. Xu, W. Liu, N. Hao, and Y. Wang, *ArXiv:1106.5169* (2011).
- [61] J. Zhao, W. Ratcliff, J. W. Lynn, G. F. Chen, J. L. Luo, N. L. Wang, J. P. Hu, and P. C. Dai, *Physical Review B* **78**, (2008).
- [62] C. Fang, H. Yao, W. F. Tsai, J. P. Hu, and S. A. Kivelson, *Physical Review B* **77**, (2008).
- [63] Y. K. Luo, Q. Tao, Y. K. Li, X. Lin, L. J. Li, G. G. Cao, Z. A. Xu, Y. Xue, H. Kaneko, A. V. Savinkov, et al., *Physical Review B* **80**, (2009).
- [64] L. W. Harriger, A. Schneidewind, S. L. Li, J. Zhao, Z. C. Li, W. Lu, X. L. Dong, F. Zhou, Z. X. Zhao, J. P. Hu, et al., *Physical Review Letters* **103**, (2009).
- [65] Y. Zhang, L. X. Yang, M. Xu, Z. R. Ye, F. Chen, C. He, H. C. Xu, J. Jiang, B. P. Xie, J. J. Ying, et al., *Nature Materials* **10**, 273 (2011).
- [66] X.-P. Wang, T. Qian, P. Richard, P. Zhang, J. Dong, H.-D. Wang, C.-H. Dong, M.-H. Fang, and H. Ding, *Europhysics Letters* **93**, 57001 (2011).
- [67] D. Mou, S. Liu, X. Jia, J. He, Y. Peng, L. Zhao, L. Yu, G. Liu, S. He, X. Dong, et al., *Physical Review Letters* **106**, 107001 (2011).
- [68] W. Bao, Q.-Z. Huang, G.-F. Chen, M. A. Green, D.-M. Wang, J.-B. He, and Y.-M. Qiu, *Chinese Physics Letters* **28**, 6104 (2011).
- [69] W. Bao, G. N. Li, Q. Huang, G. F. Chen, J. B. He, M. A. Green, Y. Qiu, D. M. Wang, and J. L. Luo, *Arxiv:1102.3674* (2011).
- [70] M. Wang, C. Fang, D.-X. Yao, G. Tan, L. W. Harriger, Y. Song, T. Netherton, C. Zhang, M. Wang, M. B. Stone, et al., *arXiv:1105.4676* (2011).
- [71] S. L. Li, C. de la Cruz, Q. Huang, Y. Chen, J. W. Lynn, J. P. Hu, Y. L. Huang, F. C. Hsu, K. W. Yeh, M. K. Wu, et al., *Physical Review B* **79**, (2009).
- [72] F. Chen, B. Zhou, Y. Zhang, J. Wei, H. W. Ou, J. F. Zhao, C. He, Q. Q. Ge, M. Arita, K. Shimada, et al., *Physical Review B* **81**, (2010).
- [73] C. Fang, B. A. Bernevig, and J. P. Hu, *Epl* **86**, (2009).
- [74] C. Fang, B. Xu, P. Dai, T. Xiang, and J. Hu, *Arxiv:1103.4599* (2011).
- [75] C. Xu and J. Hu, *0903.4477* (2009).